

High-efficiency deflection of high energy protons due to channeling along the $\langle 110 \rangle$ axis of a bent silicon crystal

W. Scandale^{a,b,c}, G. Arduini^a, M. Butcher^a, F. Cerutti^a, M. Garattini^a, S. Gilardoni^a, A. Lechner^a, R. Losito^a, A. Masi^a, D. Mirarchi^a, S. Montesano^a, S. Redaelli^a, R. Rossi^{a,c}, P. Schoofs^a, G. Smirnov^a, G. Valentino^a, D. Breton^b, L. Burmistrov^b, V. Chaumat^b, S. Dubos^b, J. Maalmi^b, V. Puill^b, A. Stocchi^b, E. Bagli^c, L. Bandiera^c, G. Germogli^c, V. Guidi^c, A. Mazzolari^c, S. Dabagov^d, F. Murtas^d, F. Addesa^{a,c}, G. Cavoto^e, F. Iacoangeli^e, F. Galluccio^f, A.G. Afonin^g, Yu.A. Chesnokov^g, A.A. Durum^g, V.A. Maisheev^g, Yu.E. Sandomirskiy^g, A.A. Yanovich^g, A.D. Kovalenko^h, A.M. Taratin^h, A. S. Denisovⁱ, Yu.A. Gavrikovⁱ, Yu.M. Ivanovⁱ, L.P. Lapinaⁱ, L. G. Malyarenkoⁱ, V.V. Skorobogatovⁱ, T. James^j, G. Hall^j, M. Pesaresi^j, M. Raymond^j

^aCERN, European Organization for Nuclear Research, CH-1211 Geneva 23, Switzerland

^bLaboratoire de l'Accelérateur Lineaire (LAL), Université Paris Sud Orsay, Orsay France

^cINFN Sezione di Ferrara and Dipartimento di Fisica e Scienze della Terra, Università di Ferrara, Via Saragat 1 Blocco C, 44121 Ferrara, Italy

^dINFN LNF, Via E. Fermi, 40 00044 Frascati (Roma) Italy

^eINFN Sezione di Roma, Piazzale Aldo Moro 2, 00185 Rome, Italy

^fINFN Sezione di Napoli, Italy

^gInstitute for High Energy Physics in National Research Centre "Kurchatov Institute", 142281, Protvino, Russia

^hJoint Institute for Nuclear Research, Joliot-Curie 6, 141980, Dubna, Russia

ⁱPetersburg Nuclear Physics Institute in National Research Centre "Kurchatov Institute", 188300, Gatchina, Russia

^jImperial College, London, United Kingdom

Abstract

A deflection efficiency of about 61 % was observed for 400 GeV/c protons due to channeling, most strongly along the $\langle 110 \rangle$ axis of a bent silicon crystal. It is comparable with the deflection efficiency in planar channeling and considerably larger than in the case of the $\langle 111 \rangle$ axis. The measured probability of inelastic nuclear interactions of protons in channeling along the $\langle 110 \rangle$ axis is only about 10 % of its amorphous level whereas in channeling along the $\langle 110 \rangle$ planes it is about 25 %. High efficiency deflection and small beam losses make this axial orientation of a silicon crystal a useful tool for the beam steering of high energy charged particles.

Keywords: Crystal; channeling; beam deflection

1. Introduction

In the last twenty years, channeling has been exploited exploited for steering [1], collimation [2, 3, 4] and extraction [2, 5, 6, 7] of relativistic beams in circular accelerators, as well as splitting and focusing of extracted beams [8]. In the last decade, a significant boost to the research on particle-crystal interactions was provided by the fabrication of uniformly bent crystals with thickness along the beam direction suitable for experiments at high-energy. The novel generation of crystals has demonstrated the capability of efficiently steering positively charged [9, 10] particle beams and to observe the deflection of negatively charged particle beams [11, 12]. As well as efficient deflection, channeling has been shown to modify the probability of incoherent interactions with atomic nuclei with respect to an amorphous material of the same length [13]. In particular, the use of bent crystals as a primary collimator has been demonstrated to reduce the beam losses in the SPS proton synchrotron at CERN [14, 15, 16], leading to the installation of two bent crystals in the LHC collider [17]. The crystals installed in the LHC were successfully tested and shown to reduce the beam losses in the LHC ring with 6.5 TeV/c protons [18].

As a charged particle traverses a crystal with a small angle

with respect to one of the main crystallographic axes, the particle motion is governed by the potential of the atomic strings averaged along the axis [19], i.e. the particle is subject to axial channeling (AC). The maximum angle between the particle incident angle and the crystal axis, for which channeling occurs is called critical angle for channeling $\psi_{ac} = (4Ze^2/p\beta d)$ [19], where d is the distance between neighboring atoms in the atomic string, $p\beta$ the particle momentum-velocity, Z the atomic number of the crystal atoms and e the elementary charge. For a silicon crystal, ψ_{ac} is almost three times larger than the critical angle for channeling between atomic planes, i.e. planar channeling (PC) [20]. However, because the potential barrier separating the axial channels formed by neighboring atomic strings is rather low, the fraction of particles confined within a single axial channel is limited. As an example, for a silicon crystal, such a potential barrier is ~ 6 eV for the $\langle 110 \rangle$ direction and only 1 eV for the $\langle 111 \rangle$. If a particle under AC has a transverse energy slightly higher than the potential well barrier, particles interacting with a bent crystal may be deflected by the multiple scattering on the atomic strings toward the bending direction, increasing the efficiency of AC. Indeed, as soon as a particle penetrates the crystal, the position of scattering centers shifts,

causing the subsequent random scattering with atomic strings to acquire a preferential direction. Such an effect was experimentally demonstrated for positively [10, 21] and negatively [12] charged particles.

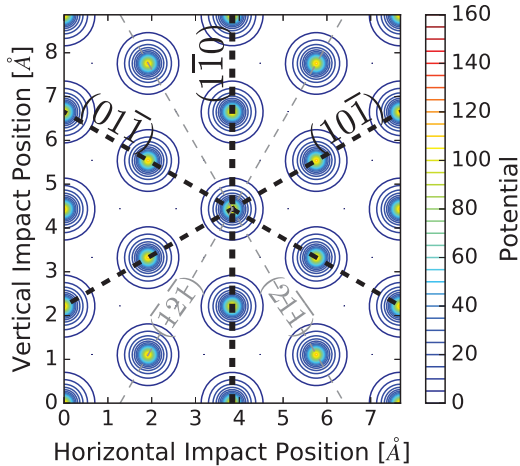


Figure 1: Potential averaged along the $\langle 111 \rangle$ axis of a silicon crystal. The directions of the (110) and (211) planes are shown.

As predicted in [22] high deflection efficiency and small beam losses due to inelastic interactions may be achieved using the axial channeling, most strongly along the $\langle 110 \rangle$ axis of a silicon crystal. Despite that fact, experimental measurements on AC are limited to studies of the deflection efficiency of 400 GeV/c protons interacting with a $\langle 111 \rangle$ silicon crystal [10, 12, 21], and measurement of the inelastic interaction frequency (INI) under AC was observed only for 15 GeV/c pions interacting with germanium crystals [23, 24].

In this paper, we experimentally investigate the deflection efficiency and the inelastic interaction frequency of 400 GeV/c protons interacting with $\langle 111 \rangle$ and $\langle 110 \rangle$ bent silicon crystals under axial channeling at the H8 external line of the SPS at CERN.

2. AC mechanism

Charged particles interacting with an aligned crystal under AC are mainly deflected by two phenomena, hyperchanneling [25] and the randomization of transverse momenta of the particles because of multiple scattering by atomic strings [26]. Hyperchanneling consists in the confinement of the particle trajectory between the potential well barriers separating neighboring atomic planes. Due to the low potential barrier, such a phenomenon is possible only for a few percent of the incident particles. On the contrary, when particles scatter on atomic strings, the deflection due to the randomization of transverse particle momentum affects all the particles not under hyperchanneling and is possible if the crystal bending angle (α) is lower than a characteristic value α_{ts} [27]

$$\alpha < \alpha_{ts} = \frac{2R\psi_{ac}^2}{l_0} \quad (1)$$

where R is crystal bending radius, $l_0 = 4/(\pi^2 n d R_a \psi_{ac})$ the minimum encounter length between the incident particle and a nucleus, n being the concentration of atoms in the crystal and R_a the atomic screening radius.

Although Eq. 1 proved to be a good condition for the observation of the particle deflection due to incoherent scattering [10, 12, 21], it does not furnish an estimate of the best crystal length at a fixed bending angle. A useful parameter introduced to account for the maximum crystal length for efficient particle steering at the full bending angle $\alpha = L/R$ is the relaxation length l_r [21], i.e. the length within which the fraction of particles in the AC regime are reduced to $1/e$ and escape from AC to skew planes. In order to efficiently deflect under AC a crystal has to fulfill the inequality [21]

$$L < l_r \quad (2)$$

Up to now, an analytic equation for the calculation of l_r does not exist. The dependence of the l_r on R was worked out only for a 400 GeV/c proton beam interacting with a $\langle 111 \rangle$ Si crystal [21] and included the incoherent scattering on nuclei and electrons.

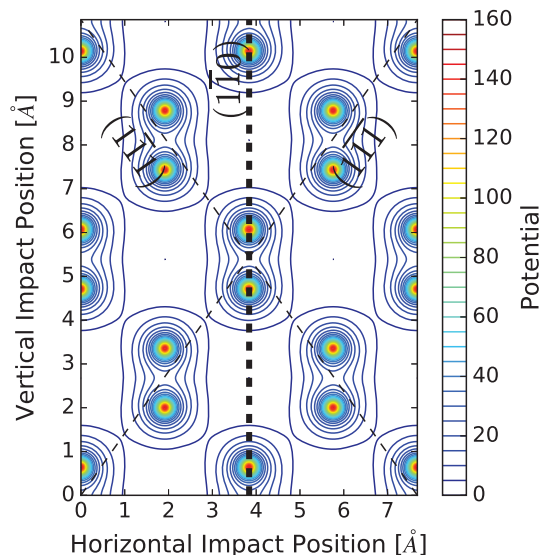


Figure 2: Potential averaged along the $\langle 110 \rangle$ axis of a silicon crystal. The directions of the (111) planes are shown.

3. Experimental measurements

The experimental setup was based on a particle telescope [28], consisting of ten planes of silicon microstrip sensors, arranged as five pairs, each measuring two orthogonal coordinates, with an active area of $3.8 \times 3.8 \text{ cm}^2$. The telescope provided excellent angular and spatial resolution for measuring the trajectories of incident and outgoing particles. The apparatus had a long baseline, of approximately 10 m in each arm, and achieved an angular resolution in the incoming arm of $2.5 \mu\text{rad}$

Table 1: Parameters of the $\langle 111 \rangle$ and $\langle 110 \rangle$ bent Si crystals, with R the crystal bending radius, L the crystal length along the beam direction, α_{pl} the channeling mean deflection angle.

	$\langle 111 \rangle$	$\langle 110 \rangle$
Plane	($\bar{1}10$)	($\bar{1}10$)
Axis	$\langle 111 \rangle$	$\langle 110 \rangle$
L (mm)	1.941 ± 0.002	1.881 ± 0.002
R (m)	32 ± 2	35 ± 2
α_{pl} (μrad)	63 ± 1	54 ± 1

and a total angular resolution on the difference of the two arms of $5.2 \mu\text{rad}$, with performance limited by multiple scattering in the sensor layers. The crystal was mounted on a high-precision goniometer with an angular resolution of about $1 \mu\text{rad}$. This instrument allowed three degrees of freedom, one linear and two rotational movements, to align the crystal along either the horizontal or vertical directions. Two pairs of scintillators were placed after the target outside the beampipe in order to measure the secondary particles produced by the nuclear interactions of protons with the silicon crystals. Pre-alignment of the samples was achieved by means of a laser system parallel to the beam direction.

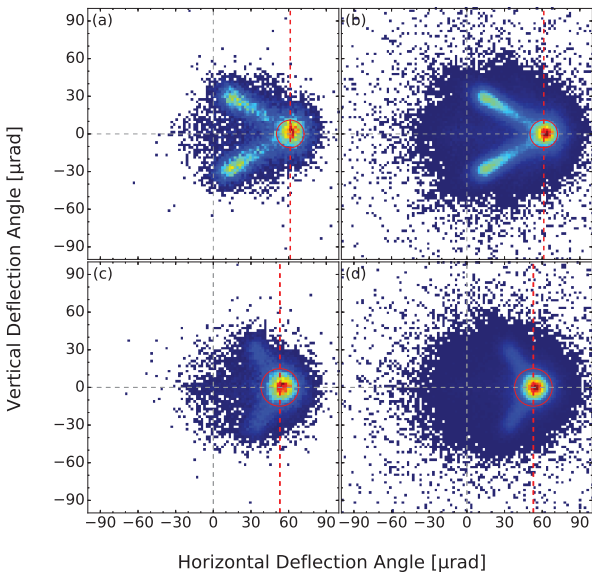


Figure 3: Experimental (a. and c.) and simulated (b. and d.) distributions of the horizontal and vertical deflection angles of 400 GeV/c protons interacting with the $\langle 111 \rangle$ (a. and b.) and $\langle 110 \rangle$ (c. and d.) crystals.

The targets were two silicon crystals produced according to the method described in Ref. [29, 30, 31]. The crystals were mounted on mechanical holders that impart a controlled deformation to the primary and the anticlasic curvatures [5, 32]. The crystal parameters are reported in Table 1. Both the crystals have a ~ 2 mm length and the same bent $\langle 1\bar{1}0 \rangle$ axis orthogonal to the beam direction. Therefore, both crystals make use of

a $\langle 1\bar{1}0 \rangle$ bent plane for PC. However, the bent axes parallel to the beam direction are different, being respectively $\langle 111 \rangle$ and $\langle 110 \rangle$. As a consequence the use of such crystals allows comparison of the AC features for two different crystal axes under the same experimental condition. The crystal torsion due to the mechanical holder was compensated in the data analysis for both the crystals [33].

The INI for a particle interacting with a crystal under AC (n_{ac}) can be expressed in units of the INI for a particle interacting with an amorphous material (n_{am}). In the experiment, we tagged as nuclear interacting particles (N_{ini}) the incoming particles that interact with the crystals and produced a signal in both the scintillators. Subtracting the background events that produce a coincidence in the scintillators ($N_{bg,ini}$) from the measurement (N_{ini}) and dividing by the events under misaligned condition minus the background events ($N_{am,ini} - N_{bg,ini}$), we obtain the INI (n) for the particles under AC:

$$n = \frac{N_{ini} - N_{bg}}{N_{am} - N_{bg}} \quad (3)$$

Table 2: The experimental and simulated deflection efficiency (ϵ_{ac}) axial channeling along the $\langle 111 \rangle$ and $\langle 110 \rangle$ silicon crystal axes.

	$\langle 111 \rangle$		$\langle 110 \rangle$	
ϵ_{ac}	Experiment	Simulation	Experiment	Simulation
	22 ± 2	24 ± 2	61 ± 2	67 ± 2

Firstly, both the crystals were oriented under PC in order to measure the efficiency (ϵ_{pl}) and the mean deflection angle (α_{pl}). The particles with an incident angle below $2 \mu\text{rad}$ with respect to the $(\bar{1}10)$ bent plane were analyzed. The maximum deflection efficiency and the average deflection angle under PC are $83 \pm 1\%$ and $63 \pm 1 \mu\text{rad}$ for the $\langle 111 \rangle$ crystal, $82 \pm 1\%$ and $54 \pm 1 \mu\text{rad}$ for the $\langle 110 \rangle$ crystal. Since the bending radii (R) for the $\langle 111 \rangle$ (32 ± 2 m) and $\langle 110 \rangle$ (35 ± 2 m) crystals are much greater than the 0.7 m critical bending radius (R_c) at 400 GeV/c [20], the minimal bending radius for which channeling is possible, the deflection efficiency under PC is expected to be the same for the two crystals [12]. The deflection efficiency under PC was evaluated as described in Ref. [34].

After the channeling was demonstrated under PC, the crystal was oriented in order to observe AC, i.e., with the crystal axis parallel to the particle incoming direction. In order to investigate AC, both the crystals have to fulfill the inequalities in Eqs. 1 and 2. The parameter l_r was estimated as ~ 2.5 mm for $R = 32$ and ~ 3.7 for $R = 35$ [21]. Although the $\langle 111 \rangle$ axis was used for the estimation, we expect a similar or better behavior for the $\langle 110 \rangle$ axis, since the potential well depth is similar and the potential well is wider (see Figs. 1 and 2). The parameter α_{ts} is $\sim 600 \mu\text{rad}$ for the $\langle 111 \rangle$ crystal and $\sim 800 \mu\text{rad}$ for the $\langle 110 \rangle$. Because $\alpha_{ts} \gg \alpha_{pl}$ and $L < l_r$ for both the crystals, we expect a high-efficiency beam deflection through AC for both of them.

The distribution of particle deflection angle after the interaction with the two crystals is shown in Fig. 3. Table 3 shows the deflection efficiency under AC. The particles with an incident angle below $3 \mu\text{rad}$ with respect to the bent axis of the two crystals were analyzed, i.e. with $\sqrt{\theta_{x0}^2 + \theta_{y0}^2} < \Theta$ where θ_{x0} and θ_{y0} are the horizontal and vertical particle incident angle with respect to the crystal axis orientation. The deflection efficiency ϵ_{ac} was evaluated as the fraction of particles in the circle centered on the mean horizontal deflection with radius $11 \mu\text{rad}$ for the $\langle 110 \rangle$ crystal and $15 \mu\text{rad}$ for the $\langle 111 \rangle$ crystal. The deflection efficiency was $22 \pm 2 \%$ for the $\langle 111 \rangle$ and $61 \pm 2 \%$ for the $\langle 110 \rangle$.

Figure 4 shows the distribution of the horizontal deflection angle for a 400 GeV/c proton beam interacting with the $\langle 111 \rangle$ and $\langle 110 \rangle$ silicon crystals. The particle with an incident angle below $3 \mu\text{rad}$ are analyzed. The efficiency of one side deflection is 97 % for the $\langle 111 \rangle$ and 98 % for the $\langle 110 \rangle$ axis orientations. For both crystals the particle distributions are symmetric on the vertical plane and skewed to positive values on the horizontal plane, i.e. the bent plane. Although all the particles are initially subject to AC a consistent fraction is captured by the skew planes that intersect the main axis. For the crystal offering the $\langle 111 \rangle$ axis the two symmetric tails that belong to the $\langle 110 \rangle$ family of planes at 60° from the main $\langle 111 \rangle$ plane (see Figs. 1 and 4), leading the particles captured by them to be deflected at an angle much lower than the full bending angle. For the crystal offering the $\langle 110 \rangle$ axis the angle between the two symmetric $\langle 111 \rangle$ planes and the main $\langle 110 \rangle$ plane is only 35.26° , causing the captured particles to be deflected at an angle similar to the main bending angle (see Figs. 2 and 4). As a consequence the deflection efficiency ϵ_{ac} is higher for the $\langle 110 \rangle$ crystal than for the $\langle 111 \rangle$.

The INI probability was measured for the axial and for amorphous (AM) orientations of the crystals. Fig. 5 shows the INI normalized to the AM condition as a function of an angular range $\pm\Theta$ around around the best AC position for both the crystals, i.e. $\sqrt{\theta_{x0}^2 + \theta_{y0}^2} < \Theta$. Particles under AM experience the same INI independently of Θ , because in such a case the crystal acts as an amorphous material. On the contrary, the INI for AC strongly depends on Θ . Indeed, as soon as the integration angle grows, the fraction of particles under AC diminishes in the beam, leading to the growing of the average INI.

The interaction frequency under PC is always higher than for AC. Indeed, as predicted in [22], the particles under AC impinge on the strong electromagnetic field of the atomic rows without approaching close to the nuclei until they are aligned with respect to the crystal axis within one ψ_{ac} . Since $\psi_{ac} \gg \psi_{pc}$ for both $\langle 111 \rangle$ and $\langle 110 \rangle$ axes ($U_{0,ac} \sim 100 \text{ eV}$ for $\langle 111 \rangle$ and $\langle 110 \rangle$ axes and $U_{0,pc} \sim 20$ for $\langle 110 \rangle$ plane), the INI under AC remains lower than the INI under PC for higher incident angles, resulting in a net reduction of the INI for the whole incident beam.

Whilst the potential well depth for $\langle 111 \rangle$ and $\langle 110 \rangle$ axes are similar, the shapes of the potential well are different. Indeed, the potential well for the $\langle 110 \rangle$ axis is much wider than the potential well for the $\langle 111 \rangle$ axis (see Fig. 2 and 1). As con-

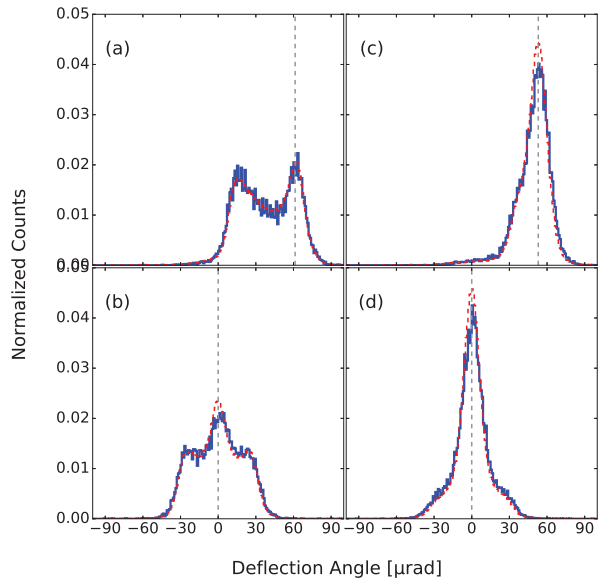


Figure 4: Distributions of horizontal (a. and c.) and vertical (b. and d.) deflection angles for a narrow fraction of the 400 GeV/c proton beam after the passage through the $\langle 111 \rangle$ (a. and b.) and $\langle 110 \rangle$ (c. and d.) silicon crystals. Continuous blue lines are the experimental data, red dashed lines are the Geant4 simulations.

sequence, the fraction of particles captured in the skew planes is $\sim 45 \%$ for $\langle 111 \rangle$ and $\sim 15 \%$ for the $\langle 110 \rangle$. The INI under AC is ~ 0.30 for the $\langle 111 \rangle$ axis and ~ 0.10 for the $\langle 110 \rangle$ axis for particles with $\sqrt{\theta_{x0}^2 + \theta_{y0}^2} < 5 \mu\text{rad}$ (see Fig. 5).

4. Monte Carlo simulations

The investigation of the trajectories inside the crystals was carried out by means of the Geant4 Monte Carlo toolkit [35]. The experimental setup at the H8-SPS area is reproduced in the simulation in order to take into account the error due to the finite resolution of the telescope. Channeling is implemented by including DYNECHARM++ [36] and ECHARM [37] into the Geant4 channeling package [38]. Simulations of the INI are shown in Fig. 5 and of the distribution of the deflection angle in Figs. 3 and 4.

The distribution of the deflection angles reproduce the experimental results. Indeed, the spot of the particles deflected by the AC and the tails filled by the particles captured by skew planes are visible. Table 3 reports the simulation results for the deflection efficiency under AC. The efficiency is slightly higher than the experimental results for both the crystals. As a consequence, the INI of the simulation is slightly lower than the experimental results.

The good agreement between the Geant4 simulations and the experimental data allows investigation of the dynamics of the interaction with the Monte Carlo approach. Since the simulations with Geant4 takes into consideration the whole experimental setup and the contribution of the multiple scattering on

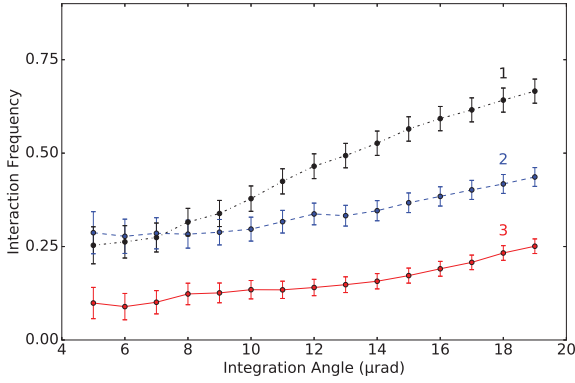


Figure 5: Measured inelastic nuclear interaction frequency (INI) of 400 GeV/c protons interacting with the $\langle 111 \rangle$ and $\langle 110 \rangle$ crystals as a function of the angular region around the $\langle 110 \rangle$ planar channeling (black dash-dotted line, 1), the $\langle 111 \rangle$ axial channeling (blue dashed line, 2) and $\langle 110 \rangle$ (red continuous line, 3) orientations. The values are normalized to the INI frequencies for the amorphous crystal orientation.

the beam line elements to the final results, a different Monte Carlo approach can be used to evaluate the deflection efficiency under AC under ideal conditions. Therefore, Monte Carlo simulations using the binary collision model were carried out. Simulations show that the deflection efficiencies may reach values of about 50 % and 80 % for the $\langle 111 \rangle$ and $\langle 110 \rangle$ axial orientations of the silicon crystals, respectively, with a narrow beam.

5. Conclusions

In summary, we compared the deflection efficiency and INI under AC of $\langle 111 \rangle$ and $\langle 110 \rangle$ axes. The experiment confirms the theoretical predictions proposed in [22] and paves the way to the use of AC as an efficient manipulator of charged particle beams.

The AC with $\langle 110 \rangle$ and $\langle 111 \rangle$ silicon crystals causes 90 % of the particles to be one side deflected. The particles captured by the skew planes (~ 15 %) for the $\langle 110 \rangle$ axis acquire a deflection angle similar to α , while while the two most strongly acting $\langle 110 \rangle$ planes of the $\langle 111 \rangle$ axis cause a considerable fraction (~ 45 %) of the particles to be deflected at an angle lower than α but > 0 . Moreover, binary collision simulations show an 80 % deflection efficiency for the $\langle 110 \rangle$ axis if we consider only the particle-crystal interaction.

The measurement allowed to clearly establish that the INI probability for particles under AC is significantly lower than for particles under PC. Moreover, we observed that the INI probability for particles under AC for a $\langle 110 \rangle$ crystal is three times lower than for a $\langle 111 \rangle$ crystal. The experimental measurements were systematically compared with Monte Carlo simulations worked out via the Geant4 toolkit. The simulations reproduced the distributions of deflection angle for both crystals, confirming the understanding of the physics behind AC. Thanks to its deflection efficiency and the low INI probability, we experimentally demonstrated that AC along the most effective $\langle 110 \rangle$ axis

of a bent silicon crystal is a good candidate for beam manipulation at high energy.

Acknowledgment

We wish to acknowledge the strong support of the CERN LHC Collimation Project. The CERN BE-OP was in charge of setting-up the H8 beam line, during the data taking. The Imperial College group gratefully acknowledges support from the UK Science and Technology Facilities Council. The PNPI and the IHEP teams wish to acknowledge support by the Russian Foundation for Basic Research Grants 05-02-17622 and 06-02-16912, the RF President Foundation Grant SS-1633.2014.2, the “LHC Program of Presidium of Russian Academy of Sciences”, the grant RFBR-CERN 12-02-91532. F. Addesa, E. Bagli, L. Bandiera, G. Cavoto and F. Iacoangeli of the INFN team were supported by ERC Ideas Consolidator Grant n. 615089 “CRY-S-BEAM”. D. Mirarchi was partially supported by the EuCARD program GA 227579, within the “Collimators and Materials for high power beams” work package (Colmat-WP).

References

- [1] A. F. Elishev *et al.*, Steering of charged particle trajectories by a bent crystal, Phys. Lett. B 88 (1979) 387 – 391. doi:10.1016/0370-2693(79)90492-1.
- [2] A. G. Afonin *et al.*, High-efficiency beam extraction and collimation using channeling in very short bent crystals, Phys. Rev. Lett. 87 (2001) 094802. doi:10.1103/PhysRevLett.87.094802.
- [3] R. P. Filler *et al.*, Rhic crystal collimation, Nucl. Instrum. Methods Phys. Res., Sect. B 234 (2005) 47 – 56. doi:10.1016/j.nimb.2005.03.004.
- [4] R. Carrigan Jr. *et al.*, Accelerator Physics at the Tevatron Collider, Springer, 2014.
- [5] Afonin, A.G. *et al.*, First results of experiments on high-efficiency single-crystal extraction of protons from the u-70 accelerator, Journal of Experimental and Theoretical Physics Letters 67 (10) (1998) 781–785. doi:10.1134/1.567748.
- [6] R. A. Carrigan *et al.*, Beam extraction studies at 900 gev using a channeling crystal, Phys. Rev. ST Accel. Beams 5 (2002) 043501. doi:10.1103/PhysRevSTAB.5.043501.
- [7] H. Akbari *et al.*, First results on proton extraction from the cern-sps with a bent crystal, Physics Letters B 313 (3) (1993) 491 – 497.
- [8] A.S. Denisov *et al.*, First results from a study of a 70 gev proton beam being focused by a bent crystal, Nucl. Instrum. Methods Phys. Res., Sect. B 69 (1992) 382 – 384. doi:10.1016/0168-583X(92)96034-V.
- [9] W. Scandale *et al.*, High-efficiency volume reflection of an ultrarelativistic proton beam with a bent silicon crystal, Phys. Rev. Lett. 98 (2007) 154801. doi:10.1103/PhysRevLett.98.154801.
- [10] W. Scandale *et al.*, Volume reflection dependence of 400 gev/c protons on the bent crystal curvature, Phys. Rev. Lett. 101 (2008) 234801. doi:10.1103/PhysRevLett.101.234801.
- [11] W. Scandale *et al.*, Observation of channeling and volume reflection in bent crystals for high-energy negative particles, Phys. Lett. B 681 (3) (2009) 233 – 236. doi:10.1016/j.physletb.2009.10.024.
- [12] W. Scandale *et al.*, High-efficiency deflection of high-energy negative particles through axial channeling in a bent crystal, Phys. Lett. B 680 (4) (2009) 301 – 304. doi:10.1016/j.physletb.2009.09.009.
- [13] W. Scandale *et al.*, Probability of inelastic nuclear interactions of high-energy protons in a bent crystal, Nucl. Instrum. Methods Phys. Res., Sect. B 268 (2010) 2655 – 2659. doi:10.1016/j.nimb.2010.07.002.
- [14] W. Scandale *et al.*, First results on the sps beam collimation with bent crystals, Phys. Lett. B 692 (2) (2010) 78 – 82. doi:10.1016/j.physletb.2010.07.023.
- [15] W. Scandale *et al.*, Comparative results on collimation of the sps beam of protons and pb ions with bent crystals, Phys. Lett. B 703 (5) (2011) 547 – 551. doi:10.1016/j.physletb.2011.08.023.

- [16] W. Scandale *et al.*, Strong reduction of the off-momentum halo in crystal assisted collimation of the sps beam, *Phys. Lett. B* 714 (2012) 231 – 236. doi:10.1016/j.physletb.2012.07.006.
- [17] W. Scandale *et al.*, Letter of Intent for an experiment at LHC (CERN), 10 June 2011.
- [18] W. Scandale, G. Arduini, M. Butcher, F. Cerutti, M. Garattini, S. Giardoni, A. Lechner, R. Losito, A. Masi, D. Mirarchi, S. Montesano, S. Redaelli, R. Rossi, P. Schoofs, G. Smirnov, G. Valentino, D. Breton, L. Burmistrov, V. Chaumat, S. Dubos, J. Maalmi, V. Puill, A. Stocchi, E. Bagli, L. Bandiera, G. Germogli, V. Guidi, A. Mazzolari, S. Dabagov, F. Murtas, F. Addesa, G. Cavoto, F. Iacoangeli, L. Ludovici, R. Santacesaria, P. Valente, F. Galluccio, A. Afonin, Y. Chesnokov, A. Durum, V. Maishev, Y. Sandomirskiy, A. Yanovich, A. Kovalenko, A. Taratin, A. Denisov, Y. Gavrikov, Y. Ivanov, L. Lapina, L. Malyarenko, V. Skrobogotov, T. James, G. Hall, M. Pesaresi, M. Raymond, Observation of channeling for 6500 gev/c protons in the crystal assisted collimation setup for {LHC}, *Physics Letters B* 758 (2016) 129 – 133. doi:http://dx.doi.org/10.1016/j.physletb.2016.05.004.
- [19] J. Lindhard, Influence of crystal lattice on motion of energetic charged particles, *Danske Vid. Selsk. Mat. Fys. Medd.* 34 (1965) 14.
- [20] V. M. Biryukov, Y. A. Chesnekov, V. I. Kotov, *Crystal Channeling and Its Applications at High-Energy Accelerators*, Springer, 1996.
- [21] L. Bandiera, A. Mazzolari, E. Bagli, G. Germogli, V. Guidi, A. Sytov, I. V. Kirillin, N. F. Shul'ga, A. Berra, D. Lietti, M. Prest, D. Salvador, E. Vallazza, Relaxation of axially confined 400 gev/c protons to planar channeling in a bent crystal, *The European Physical Journal C* 76 (2) (2016) 1–6. doi:10.1140/epjc/s10052-016-3899-x.
- [22] Y. Chesnokov, I. Kirillin, W. Scandale, N. Shul'ga, V. Truten', About the probability of close collisions during stochastic deflection of positively charged particles by a bent crystal, *Physics Letters B* 731 (2014) 118 – 121. doi:http://dx.doi.org/10.1016/j.physletb.2014.02.024.
- [23] S. Andersen, H. Esbensen, O. Fich, J. Golovchenko, H. Nielsen, H. Schiott, E. Uggerhoj, C. Vraast-Thomsen, G. Charpak, G. Petersen, F. Sauli, J. Ponpon, R. Siffert, Nuclear interactions for 15 gev/c protons and pions under random and channeling conditions in germanium single crystals, *Nuclear Physics B* 144 (1) (1978) 1 – 21. doi:http://dx.doi.org/10.1016/0550-3213(78)90496-0.
- [24] R. Carrigan, B. Chrisman, T. Toohig, W. Gibson, I.-J. Kim, C. Sun, Z. Guzik, T. Nigmanov, E. Tsyganov, A. Vodopianov, M. Hasan, A. Kanofsky, R. Allen, J. Kubic, D. Stork, A. Watson, Modulation of nuclear interactions using channeling at multi-hundred gev energies, *Nuclear Physics B* 163 (1980) 1 – 20. doi:http://dx.doi.org/10.1016/0550-3213(80)90387-9.
- [25] Barrett, J. H. *et al.*, *Hyperchanneling*, Springer US, Boston, MA, 1975, pp. 645–668.
- [26] N. Shul'ga, A. Greenenko, Multiple scattering of ultrahigh-energy charged particles on atomic strings of a bent crystal, *Physics Letters B* 353 (2) (1995) 373 – 377. doi:http://dx.doi.org/10.1016/0370-2693(95)00496-8.
- [27] I. K. NF Shul'ga, V. Truten, Stochastic mechanism of a high-energy charged-particle beam deflection by a bent crystal, *Nuovo Cim. C* 43 (2011) 425.
- [28] M. Pesaresi, W. Ferguson, J. Fulcher, G. Hall, M. Raymond, M. Ryan, O. Zorba, Design and performance of a high rate, high angular resolution beam telescope used for crystal channeling studies, *Journal of Instrumentation* 6 (04) (2011) P04006.
- [29] V. Guidi *et al.*, Tailoring of silicon crystals for relativistic-particle channeling, *Nuclear Instruments and Methods in Physics Research Section B: Beam Interactions with Materials and Atoms* 234 (2005) 40 – 46. doi:http://dx.doi.org/10.1016/j.nimb.2005.01.008.
- [30] S. Baricordi *et al.*, Optimal crystal surface for efficient channeling in the new generation of hadron machines, *Applied Phys. Lett.* 91 (6) (2007) 061908. doi:10.1063/1.2768200.
- [31] S. Baricordi *et al.*, Shaping of silicon crystals for channelling experiments through anisotropic chemical etching, *J. Phys. D* 41 (24) (2008) 245501.
- [32] V. Guidi, L. Lanzoni, A. Mazzolari, Study of anticlastic deformation in a silicon crystal for channeling experiments, *Journal of Applied Physics* 107 (11) (2010) 113534. doi:10.1063/1.3372722.
- [33] S. Hasan, Experimental techniques for deflection and radiation studies with bent crystals, Ph.D. thesis, University of Insubria (2011).
- [34] W. Scandale *et al.*, Deflection of 400 gev/c proton beam with bent silicon crystals at the cern super proton synchrotron, *Phys. Rev. ST Accel. Beams* 11 (2008) 063501. doi:10.1103/PhysRevSTAB.11.063501.
- [35] S. Agostinelli *et al.*, Geant4 simulation toolkit, *Nuclear Instruments and Methods in Physics Research Section A: Accelerators, Spectrometers, Detectors and Associated Equipment* 506 (3) (2003) 250 – 303. doi:http://dx.doi.org/10.1016/S0168-9002(03)01368-8.
- [36] E. Bagli and V. Guidi, Dynecharm++: a toolkit to simulate coherent interactions of high-energy charged particles in complex structures, *Nuclear Instruments and Methods in Physics Research Section B: Beam Interactions with Materials and Atoms* 309 (0) (2013) 124 – 129. doi:http://dx.doi.org/10.1016/j.nimb.2013.01.073.
- [37] E. Bagli, V. Guidi, V. A. Maishev, Calculation of the potential for interaction of particles with complex atomic structures, *Phys. Rev. E* 81 (2010) 026708. doi:10.1103/PhysRevE.81.026708.
- [38] Bagli, E., Asai, M., Brandt, D., Dotti, A., Guidi, V., Wright, D. H., A model for the interaction of high-energy particles in straight and bent crystals implemented in geant4, *Eur. Phys. J. C* 74 (8) (2014) 2996. doi:10.1140/epjc/s10052-014-2996-y.